Lab on a Chip

PAPER

View Article Online
View Journal | View Issue

Cite this: *Lab Chip*, 2015, **15**, 1852

Digital microfluidics for time-resolved cytotoxicity studies on single non-adherent yeast cells†

P. T. Kumar,‡[a] K. Vriens,‡[b] M. Cornaglia,[c] M. Gijs,[c] T. Kokalj,[ad] K. Thevissen,[b] A. Geeraerd,[a] B. P. A. Cammue,*[be] R. Puers[f] and J. Lammertyn*[a]

Received 15th December 2014,
Accepted 10th February 2015

DOI: 10.1039/c4lc01469c

www.rsc.org/loc

Single cell analysis (SCA) has gained increased popularity for elucidating cellular heterogeneity at genomic, proteomic and cellular levels. Flow cytometry is considered as one of the most widely used techniques to characterize single cell responses; however, its inability to analyse cells with spatio-temporal resolution poses a major drawback. Here, we introduce a digital microfluidic (DMF) platform as a useful tool for conducting studies on isolated yeast cells in a high-throughput fashion. The reported system exhibits (i) a microwell array for trapping single non-adherent cells by shuttling a cell-containing droplet over the array, and allows (ii) implementation of high-throughput cytotoxicity assays with enhanced spatio-temporal resolution. The system was tested for five different concentrations of the antifungal drug Amphotericin B, and the cell responses were monitored over time by time lapse fluorescence microscopy. The DMF platform was validated by bulk experiments, which mimicked the DMF experimental design. A correlation analysis revealed that the results obtained on the DMF platform are not significantly different from those obtained in bulk; hence, the DMF platform can be used as a tool to perform SCA on non-adherent cells, with spatio-temporal resolution. In addition, no external forces, other than the physical forces generated by moving the droplet, were used to capture single cells, thereby avoiding cell damage. As such, the information on cellular behaviour during treatment could be obtained for every single cell over time making this platform noteworthy in the field of SCA.

Introduction

In a cell population, differential responses towards external perturbations are ubiquitous, which indicates cellular heterogeneity at genomic and functional levels.[1] To elucidate information concerning cellular heterogeneity within a specific population, analysis of single cells within this population needs to be performed. Depending on the growth cultures, cells can be categorised into adherent or non-adherent cells. Spatio-temporal studies performed on adherent cells are less tedious and complex to perform, as compared to those performed on non-adherent cells due to the free floating nature of the latter. Conventional approaches for conducting cell-based studies on non-adherent cells are usually performed in bulk, in which flow cytometry is often used to analyse the responses of single cells based on their fluorescence properties. However, the obtained data are spatially and temporally unresolved and do not allow for analysis of single cells in time and space.[2] In addition, the number of available systems for precise manipulation and retention of non-adherent cells on a defined location is limited.[3] The development of platforms that support single cell analysis of non-adherent cells with spatio-temporal resolution is therefore crucial.

Over the last two decades, channel-based microfluidics has come up with powerful strategies for confining[4] and manipulating[5] single cells within physical or chemical boundaries, while maintaining an *in vivo*-like environment. Several demonstrations have been reported in which hydrodynamic forces are implemented as a strategy for isolating cells in a microfluidic flow channel, such as integrated wall traps[6–8] and obstructions.[9–11] Alternatively, incorporation of electrical,[12] optical,[13] magnetic[14] or suction forces[15] has been demonstrated for isolating single cells, such as in dielectrophoresis (DEP)[16–18] and when using optical

[a] *BIOSYST-MEBIOS, KU Leuven, Willem de Croylaan 42, Heverlee, Belgium. E-mail: jeroen.lammertyn@biw.kuleuven.be; Fax: +3216322955; Tel: +3216321459*
[b] *Centre of Microbial and Plant Genetics, KU Leuven, Kasteelpark Arenberg 20, box 2460, 3001 Heverlee, Belgium. E-mail: bruno.cammue@biw.vib-kuleuven.be; Fax: +32 16321966; Tel: +32 16329682*
[c] *Laboratory of Microsystems, Ecole Polytechnique Fédérale de Lausanne, CH-1015 Lausanne, Switzerland*
[d] *Institute of Metals and Technology, Ljubljana, Slovenia*
[e] *Department of Plant Systems Biology, VIB, Ghent, Belgium*
[f] *MICAS-ESAT, KU Leuven, Leuven, Belgium*
† Electronic supplementary information (ESI) available. See DOI: 10.1039/c4lc01469c
‡ Both authors contributed equally to this work.

tweezers.[19,20] Lately, the concept of microfabricated well arrays has also been exploited widely in research for trapping single cells in micron-sized cavities by gravitational force and implementing cell-based studies.[21–23]

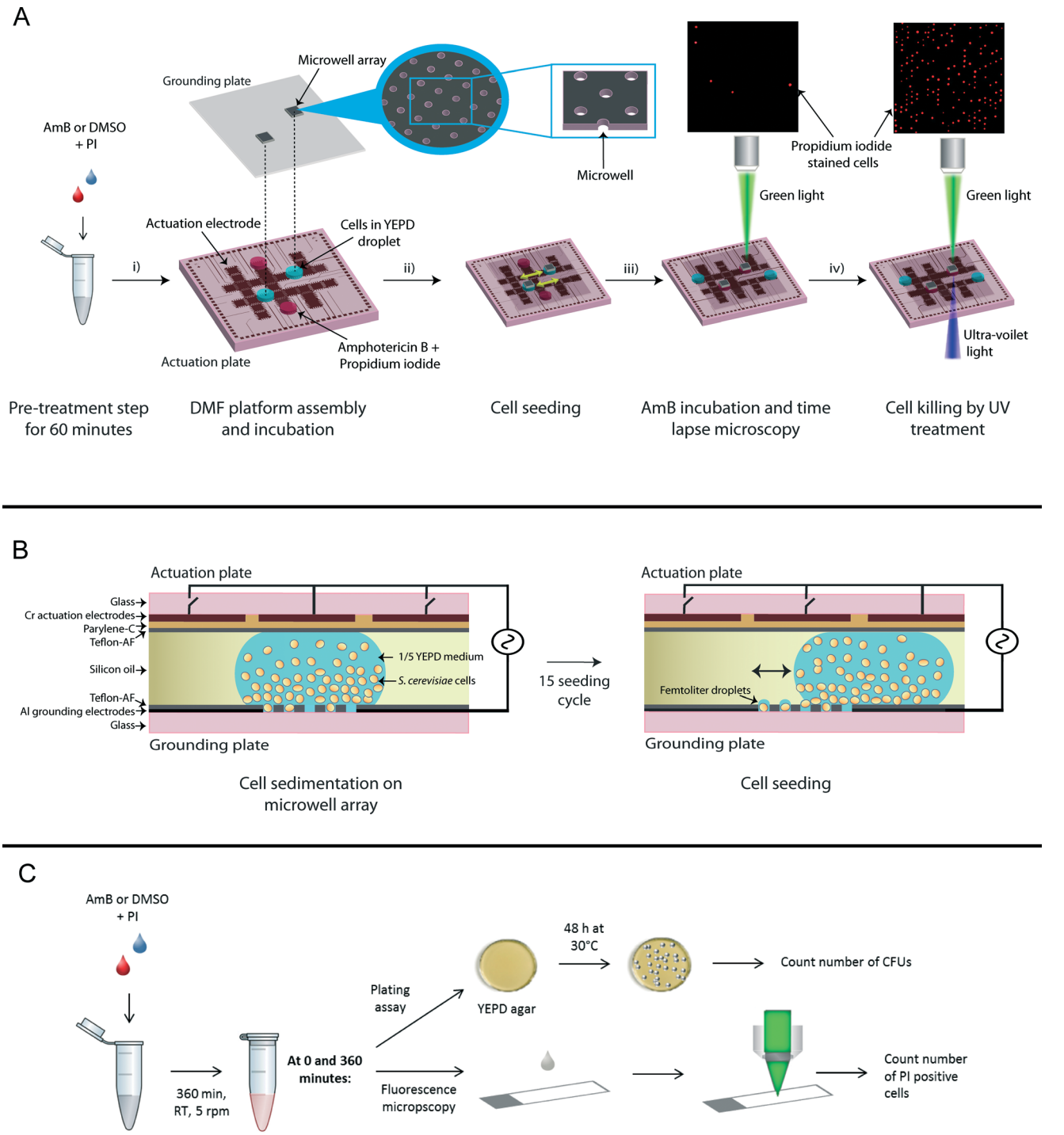

Fig. 1 Flowchart of the DMF and bulk setup used for conducting cytotoxicity assays on single *S. cerevisiae* cells. (a) The DMF platform consists of actuating and grounding plates. The latter contains two microwell arrays consisting of 22 000 microwells each for trapping single cells. After the (i) pre-treatment step with AmB or DMSO and PI, the cell droplet and the AmB droplet were added to the actuation electrodes. Then, the DMF platform was assembled, after which the cells were further incubated on the microwell array for 10 min, and (ii) cell seeding was performed. (iii) Seeded cells were subjected to treatment and the responses of single cells were monitored using time lapse fluorescence microscopy. (iv) Finally, to obtain the total number of seeded cells, the microwell array was illuminated with an intense UV beam for 20 minutes, resulting in 100% PI-positive cells. (b) Schematic overview of cell seeding on the DMF setup: cells sedimented either in between or inside the microwells; cells inside femtoliter droplets were retained inside the microwells due to the combination of drag force and surface tension. (c) The protocol that was used for conducting cytotoxicity assays in bulk, as the reference technology.

However, the current state-of-the-art technique employed for seeding single cells in channel-based microfluidics has certain drawbacks, such as the demand for high sample and reagent consumption. Moreover, the channel-constrained microfluidics is more likely to clog when a cell-rich sample is introduced.[24] Lastly, with respect to the cell-capturing system, thorough investigation and device optimization are required to avoid undesired effects such as cell stress.

Digital microfluidics (DMF) has emerged as a channel-free microfluidic technology, in which small droplets of liquid are handled on planar surfaces. It offers several advantages over channel-based microfluidics for applications where a higher degree of flexibility is required.[25] In addition to reduced reagent and sample consumption, droplets can be individually and precisely addressed through a software interface, leading to a minimal dead volume and low energy consumption. DMF technology has been demonstrated for conducting cell-based assays on adherent and non-adherent cells.[26–29] For instance, water permeability measurements were conducted on isolated *Arabidopsis thaliana* protoplasts (approx. 10–25 μm) at a single cell level by implementing an on-chip magnetic immobilization strategy.[27] In another report, an optoelectronic tweezers-integrated digital microfluidic device was used for manipulating a group of adherent HeLa cells.[26] In addition, Rival and colleagues developed an EWOD-based microfluidic chip for mRNA extraction and subsequent transcriptome analysis *via* qRT-PCR of single human HaCaT adherent cells.[28] Recently, a hybrid droplet-to-digital microfluidic system was reported, in which droplets containing single yeast cells were dispensed and monitored for growth and their ability to produce ethanol.[29] Although the number of available microfluidic systems for single cell analysis is gradually increasing, the application of DMF technology for conducting single cell studies on non-adherent cells remains rather unexplored.

In this paper, we develop a straightforward approach for real-time monitoring of single yeast cell responses during antifungal treatment in a high-throughput manner, using an electrowetting-on-dielectric (EWOD)-based DMF platform (Fig. 1A). A recently developed strategy[30] for seeding and sealing single superparamagnetic beads in femtoliter wells was extended and adjusted for trapping and subsequently analysing single yeast cells (*Saccharomyces cerevisiae*) in a microwell array. The effect of the antifungal membrane-permeabilizing agent Amphotericin B on the membrane integrity of trapped yeast cells was investigated, using the fluorescent reporter dye propidium iodide and time lapse fluorescence microscopy. This DMF platform with microwell arrays is demonstrated as a promising tool for implementing various biological applications concerning single non-adherent cells in a high-throughput manner.

Experimental

Strains and chemical reagents

Saccharomyces cerevisiae strain BY4741 was used in all experiments. Propidium iodide (PI; 540/608 nm) was supplied by Sigma Aldrich (Saint Louis, MO, USA). Amphotericin B was purchased from Sigma Aldrich (Saint Louis, MO, USA). Fluorinert FC-40 was purchased from 3M (St. Paul, MN, USA). Chemicals for photolithography, including S1818 and 351-developer, were supplied by Rohm and Haas (Marlborough, MN, USA). AZ1505 photoresist was purchased from Microchemicals GmbH (Ulm, Germany). Parylene-C dimer and Silane A174 were purchased from Plasma Parylene Coating Services (Rosenheim, Germany). Teflon-AF® was obtained from Dupont (Wilmington, DE, USA).

Design and fabrication of digital microfluidic plates

To perform a high-throughput assay, the grounding and actuation plates of the DMF platform were designed to accommodate and optically visualise two arrays, consisting of 22 000 microwells each (Fig. 1A). As such, two experiments could be conducted in parallel. Fabrication of DMF chips was performed in the ESAT-MICAS cleanroom facility of KU Leuven, as described by Witters and colleagues,[30] with some minor modifications as briefly described below.

Actuation plate. Cleaned glass wafers (1.1 mm thickness) were sputter coated with chromium (100 nm) and patterned using standard photolithographic processes. The plates were cleaned with acetone and IPA twice, and the surface was plasma activated (O_2-plasma, 150 mtorr, 100 W). To promote adhesion, the plates were primed with Silane A174 and then coated with a layer of Parylene-C (3 μm) using chemical vapour deposition. A thin layer of Teflon-AF® (approx. 200 nm thickness using 3% w/w in Fluorinert FC-40) was subsequently spin-coated (1200 rpm) on top of the Parylene-C layer, and baked for 5 min at 110 °C and 5 min at 200 °C. Crenellated actuation electrodes with dimensions of 2.8 mm × 2.8 mm were selectively actuated to manipulate individual droplets of 2.7 μL. A slight modification was made in the layout of the electrodes from the one reported in our previous studies, where the number of crossing paths between rows and columns was increased from one to two. This modification was required to improve the flexibility during droplet manipulations (Fig. 1A).

Grounding plate. The grounding plate of the DMF device was fabricated as previously described.[30] Briefly, cleaned glass wafers (1.00 mm thickness) were coated with an aluminium layer (40 nm) using thermal evaporation, leaving two 2.5 × 2.5 mm visualization windows. The surface was then coated with fluoroalkylsilane Dynasylan® F 8263, followed by spin-coating with Teflon-AF® (approx. 3 μm). The fluoroalkylsilane improved the adhesion between Teflon-AF® and aluminium. In order to pattern the microwells in the Teflon-AF® surface, a hard contact masking procedure was developed by depositing Parylene-C (1 μm) and aluminium (60–80 nm) layers. A thin layer of the AZ1505 photoresist was then spin-coated on the aluminium layer. Using standard photolithography processes, aluminium was patterned and etched. Finally, to transfer the pattern from aluminum to Teflon-AF®, the stack was subjected to O_2-plasma (150 mtorr, 100 W)

for 10 min. At last, the aluminum–Parylene-C mask was peeled off using a pair of forceps, revealing the two microwell arrays (1.9 mm × 1.9 mm) on a single grounding plate, consisting of 22 000 microwells each. The patterned microwells were measured to be approximately 5.5 μm wide and 3 μm deep, and were arranged in a hexagonal pattern with a pitch distance of 14 μm.

DMF platform operation

A double-sided tape of 160 μm thickness was applied to the actuation plate as a spacer and for adhesion of the grounding plate to the actuation plate. The assembled plates were installed in the custom-made DMF microfluidic chip holder. The actuation sequence of the electrodes was controlled with a customized Labview program (National Instruments Corp., Austin, TX, USA) and an in-house developed Matlab-based program (MathWorks Inc., Natick, MA, USA). Droplets were driven by an AC-voltage of 120–130 V_{rms}, with an activation time of 1000 ms and a relaxation time of 40 ms. The AC-actuation voltage was realized by oscillating waveforms, produced by a function generator operating at 1 kHz (GFG-8216A, ISOTECH, England) and further amplified by an amplifier (FLC Electronics A600, Sweden).

Cell culture

Saccharomyces cerevisiae strain BY4741 was used in all experiments. Reagents were supplied by Lab M Ltd. (Lancashire, England), unless stated otherwise. Media used were YEPD (1% yeast extract; 2% peptone; 2% dextrose) and 1/5 YEPD (YEPD diluted in distilled water). A yeast culture grown overnight at 200 rpm and 30 °C was diluted to an optical density (OD) of 0.15 measured at λ = 600 nm in a flask containing 50 mL of YEPD and further cultured at 200 rpm and 30 °C for 5 hours to obtain exponentially growing cells. The cells were then pelleted by centrifugation at 4000 rpm for 3 min, washed and re-suspended in 1/5 YEPD to an OD of 3.

Single cell seeding in the microwell array and cytotoxicity assay

Cell death can occur *via* either apoptotic or non-apoptotic mechanisms, depending on the influence of the stimuli on cell health.[31] One of the hallmarks of apoptosis, in contrast to non-apoptotic mechanisms, is the presence of an intact cell membrane.[32] Propidium iodide (PI) is a fluorescent dye that can enter cells with a compromised plasma membrane (*i.e.* non-apoptotic cells). In this study, we investigated the effect of the antifungal drug Amphotericin B (AmB) on these subpopulations by PI staining.

One hour prior to cell seeding in the microwell array, the yeast culture was pre-treated with AmB at final concentrations of 10 μM, 25 μM, 50 μM, 100 μM and 200 μM, in a dimethyl sulfoxide (DMSO) background of 1% (v/v), or with 1% DMSO alone (control treatment), while placed in a rotator mixer (14 rpm) (Fig. 1A, i). The off-chip pre-treatment of cells with AmB was performed for pre-loading of the cells with the drug. As membrane permeabilization events were only observed after 60 min of treatment, pre-treatment in bulk for 60 min was possible. After pre-treatment, cell seeding was performed in two steps. First, two 2.7 μL of droplets, one containing pre-treated cells and the other containing the corresponding AmB concentration and 2 μg mL^{-1} propidium iodide (PI) in 1/5 YEPD (AmB/PI), were placed on two separate electrodes of the actuation plate. Upon assembling the microwell array in the grounding plate, the array would align with the cell droplet (Fig. 1A) and sandwich it between the plates. In the next step, 80 μL of silicon oil was added in between the two plates using a pipette to prevent sticking and evaporation of the cell droplet (Fig. 1B). The assembled plates were placed in the DMF chip holder, and the holder was flipped upside down and incubated for another 10 min at room temperature to allow sedimentation of the cells. This step was followed by automated shuttling of the cell droplet over the microwell array using software-assisted EWOD actuation, referred to as seeding cycles (Fig. 1A, ii).

After seeding, the cell droplet was actuated away from the microwell array, after which the AmB/PI droplet was transported to the microwell array. The cell responses induced by AmB were monitored for the next 300 min (360 min, including the pre-treatment step) in 15 min intervals, using an inverted fluorescence microscope (IX-71, Olympus, Tokyo, Japan) equipped with a CCD camera (Fig. 1A, iii). Using a 20× lens magnification (IX-71, Olympus, Tokyo, Japan), the complete array was scanned in 9 overlapping frames in approximately 15 seconds, in which a single frame covered approximately 4100 wells. After 360 min, the total number of trapped cells was determined by exposing the array to an intense beam of UV radiation for 20 min, thereby abruptly killing and permeabilizing all the cells, rendering them PI-positive (Fig. 1A, iv).

Assessing the reproduction ability of trapped yeast cells

In order to evaluate the reproduction ability of the trapped cells after cell seeding, budding events were monitored for each trapped yeast cell. In the first step, yeast cells were seeded by employing the protocol described earlier with a minor modification; the two 2.7 μL of droplets that were placed on the electrodes consisted of a droplet containing untreated yeast cells and a droplet of 1/5 YEPD. After cell seeding, the cell droplet was actuated away from the microwell array and the 1/5 YEPD droplet was transported to the microwell array. The DMF chip was disassembled in order to carry out bright-field microscopy to monitor cell budding events, as no visualization window was present in the actuation plate and hence, budding events could not be monitored using an assembled chip. As such, solely the grounding plate was used for the remainder of the experiment and budding events were monitored for 180 min with 10 min intervals using bright-field microscopy (Zeiss Imager Z1 microscope (Carl Zeiss, Germany); AxioCam MRm camera (Carl Zeiss, Germany)). Every 60 min, 1/5 YEPD medium was added to the microwell array to compensate for the evaporation of the

droplet covering the array, as reproduction ability assays were carried out in an air environment instead of an oil environment.

Cytotoxicity assay in bulk

Exponentially growing yeast cells (OD = 3 in 1/5 YEPD) were supplemented with PI to a final concentration of 2 μg mL^{-1}. The cells were treated either with a dose of AmB (final concentration of 10 μM, 25 μM, 50 μM, 100 μM and 200 μM in 1% DMSO background) or with 1% DMSO (v/v) as control treatment. The suspension containing cells, PI and AmB in 1/5 YEPD was then transferred to Eppendorf tubes, covered with a layer of silicon oil, placed on a horizontal rotator mixer (5 rpm) and incubated in the dark at room temperature for 6 h. At the start (t_0) and the end (t_6) of the treatment, plating assay and fluorescence microscopy (540/608 nm) were performed (Fig. 1C). In the plating assay, a 10-fold dilution series of the cell suspensions was prepared in phosphate buffered saline (PBS) to obtain appropriate cell concentrations (*i.e.* 300 to 3000 cells per mL). Subsequently, appropriate cell suspensions were spread on YEPD agar plates, after which the plates were allowed to dry for 10 min and the cells were grown for 48 h at 30 °C to visualize the number of Colony Forming Units (CFUs). The CFUs were counted manually (*i.e.* growth+) and the plates containing 30 to 300 CFUs were used for further calculations. Fluorescence microscopy (Zeiss Imager Z1, Carl Zeiss AG, Oberkochen, Germany) provided the number of cells with compromised cell membranes, *i.e.* non-apoptotic cells (PI+/growth−),[32] whereas the plating assay accounted for the number of living cells (PI−/growth+) after treatment. Subtracting these fractions from 100% yielded the percentage of apoptotic cells (PI−/growth−) after treatment, which is relevant as low doses of AmB induce apoptosis in yeast.[33] Data were normalized to the control treatment.

Statistical analysis

All data were normalized to the control treatment within the same setup. In all statistics, a normal distribution of the data was assumed. A paired two-tailed Student's *t*-test was performed to evaluate the differences between the results obtained in bulk and DMF experiments after 360 min using the same concentration of AmB. A survival analysis was performed on the DMF data by using the log-rank test for trend. Asymmetrical 95% confidence intervals are plotted, as they present the true uncertainty of the number of PI-negative cells, and are therefore more valid than symmetrical 95% confidence intervals, which present the uncertainty based on a fitted model. The statistical log-rank test, followed by the Bonferroni correction to allow multiple comparisons, was used to evaluate the differences between curves,[34,35] and $P < 0.005$ was considered as statistically significant for these calculations. In all other cases, $P < 0.05$ was considered as statistically significant. Statistical analyses were performed with GraphPad Prism (GraphPad Software, Inc., CA, USA).

Results and discussion

Single cell seeding

Microwell size optimization. In order to trap single cells in the microwells, we first analysed the cell size distribution in a population of cells using flow cytometry (BD Biosciences, San Jose, CA, USA). Although the cell sizes were dispersed between 3.5–8 μm, the size of the majority of cells was between 4.5–5.5 μm and we selected this as our target size interval. In this way, either one or no cell is trapped in each microwell. To obtain reproducible feature sizes during microwell array fabrication, photolithography parameters were optimized. The effect of the exposure dosage and the development time on the pattern developed on the photoresist was studied. Non-optimal exposure and development times lead to inadequate etching or over-etching of the photoresist, resulting in too small or too big wells. Consequently during cell seeding, either no cell, single cells or multiple cells were trapped in one well. In our experiments, we used an exposure dosage of 6 mJ cm^{-2} and a development time of 45 seconds, resulting in wells with a size of 5.3 ± 0.1 μm (10 000 measurements over 4 arrays; data not shown).

Cell trapping. After assembling the DMF plates in the holder, the chip was flipped upside down to allow cell sedimentation on the microwell array. In this step, cells either entered the microwells due to gravity or sedimented in between the microwell spaces. During cell seeding, the receding droplet meniscus generated an effective drag force in combination with surface tension that manipulated the cells to enter and stay inside the microwells.[36] In addition, the hydrophilic-in-hydrophobic features, fabricated in the Teflon layer of the grounding plate, promoted cell trapping and favoured retention of cells in the microwell structures. No external forces, other than surface tension and physical forces generated by droplet movement, were used to trap single cells, thereby avoiding cell damage. The selective wetting properties of the array, combined with the surface tension generated by the receding droplet meniscus, were accountable for removing single cells that settled in between the microwells. The presence of an oil environment offered further advantages. It avoided the evaporation of the femtoliter droplets generated in the microwells, which in the absence of oil evaporated in less than a second, leading to osmotic lysis of seeded cells.[37] Moreover, YEPD is a viscous medium and droplet manipulation of YEPD on a Teflon surface in an air environment is challenging. However, on the DMF platform, manipulation of 1/5 YEPD was performed effectively in an oil environment and Teflon surface fouling was found to be greatly reduced. The use of 1/5 YEPD did not affect the behaviour of the cells, since cell division in 1/5 YEPD occurred at 112 ± 5 min (Fig. S1B†), which is in line with the literature.[38,39]

Reproduction ability of trapped yeast cells. Exposure of cells to certain physical or mechanical stresses may influence their tolerance towards antifungal agents, which might be an obstacle. To assess the stresses that the cells might have

acquired by undergoing seeding cycles on the DMF platform, the ability of the seeded cells to reproduce was analysed. In these experiments, the division time of the seeded yeast cells was considered as a measure of cell sensitivity towards external stimuli. In each experiment, at least 30 cells were monitored. The results are shown in the ESI† (Fig. S1). Although only single yeast cells are trapped during seeding, the cells can reproduce while trapped inside a microwell when growth medium is provided. Reproduction of *S. cerevisiae* is marked by budding events (*i.e.* doubling), in which the mother and daughter cell are attached to each other during growth. As such, one cell is trapped inside the microwell whereas the other cell is situated outside the well on top of the trapped cell, as shown in Fig. S1A.† Unlike on-chip antifungal treatment in which droplet manipulations were carried out in oil, assessment of the reproduction ability of trapped yeast cells was performed in an air environment. In order to negate the influence on cell viability, due to the evaporation of the droplet covering the microwell array, 1/5 YEPD medium was carefully added to the array every 60 min without affecting the location of the trapped cells. Since all cells showed reproduction ability within 180 min, all cells were defined as viable and therefore, cell viability was not affected in these experiments. The doubling time of yeast is approximately 120 min,[33,34] and when seeded cells were incubated in 1/5 YEPD, cell division occurred at 112 ± 5 min (Fig. S1B†). Hence it can be stated that the seeded cells respond in a normal way when incubated in growth medium, and therefore the DMF setup could be used to analyse cellular responses towards other external stimuli, such as antifungal drugs.

On-chip cytotoxicity assay of single yeast cells using DMF

Cytotoxicity assays were performed with different dosages of AmB and non-apoptotic cell death events were monitored using PI and fluorescence microscopy. To improve the throughput of the system, the complete array was imaged in a scanning mode. AmB is a widely used antifungal drug that primarily kills yeast cells either *via* ergosterol binding or *via* channel-mediated membrane permeabilization.[40] AmB can induce cell death either *via* necrosis, a type of non-apoptosis in which cells die with a compromised cell membrane, or *via* apoptosis or programmed cell death.[33] In this study, we analysed the fraction of these two subpopulations in a yeast culture treated with different AmB concentrations over time using the DMF platform. In DMF experiments, an average of 1200 cells was monitored over a period of 360 min at single cell resolution, which corresponded to a seeding efficiency of 5.75 ± 3.14%. The average number of seeded cells was sufficient for conducting biology-related studies in a high-throughput fashion, since a higher number of cells was monitored on-chip as compared to that found in equivalent bulk experiments, in which at least 100 cells were monitored. One of the hallmarks of apoptosis, in contrast to necrosis, is the presence of an intact cell membrane.[32] PI is a fluorescent dye that enters cells with a compromised plasma membrane, and is therefore used as a marker for non-apoptotic cell death. After cell entry, PI irreversibly binds to the nucleus.[41] Incubation of untreated yeast cells with PI for 6 h did not affect cell viability (data not shown) and thus did not affect the results obtained in this study.

Fig. 2A shows that AmB induced non-apoptotic cell death in a dose-dependent manner. In Fig. 2B, a survival analysis of the DMF dataset is given, which was performed to evaluate whether treatment of cells with different AmB dosages affects non-apoptotic cell death events in a significant manner. A higher dose of AmB (200 μM) induced membrane permeabilization more rapidly than lower AmB dosages, as illustrated by a decreased median survival; 50% non-apoptotic cell death was reached at 210 min when cells were treated with 200 μM AmB, whereas a median survival of 270 min was

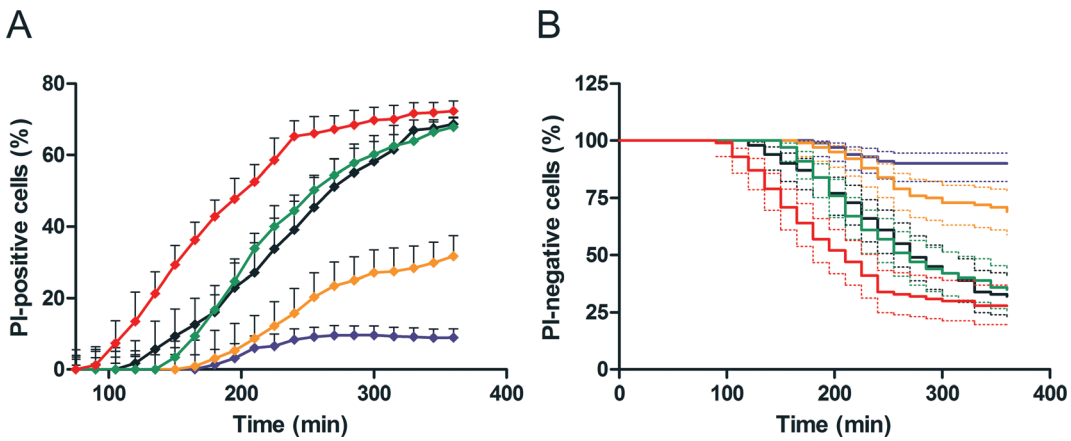

Fig. 2 Analysis of non-apoptotic cell death during AmB treatment on the DMF platform. Yeast cells were treated with different dosages of AmB displayed by coloured lines, *i.e.* 10 μm (blue), 25 μm (orange), 50 μm (black), 100 μm (green) and 200 μm (red), and monitored for membrane permeabilization events (*i.e.* PI-positive cells, indicative of non-apoptotic cell death) for 6 hours in 15 min intervals using time lapse fluorescence microscopy. (a) Representation of the cumulative amount of PI-positive cells over time. Means and standard errors of the mean (sems) (n = 4 independent biological repetitions) are presented. To avoid overcrowding of the figure, only the above fractions of the sems are plotted. (b) Survival analysis of DMF results to determine whether treatment of cells with different dosages of AmB affects non-apoptotic cell death events in a significant manner. Dotted lines represent asymmetrical 95% confidence intervals.

observed for treatment with 50 μM and 100 μM AmB. Fifty percent non-apoptotic cell death was not reached with AmB dosages lower than 50 μM within the time frame of the experiments. Significant differences between curves were analysed by employing the log-rank test, followed by the Bonferroni correction to allow multiple comparisons. The number of comparisons was 10 and therefore, a threshold of $P < 0.005$ was considered statistically significant. Although no significant differences were found between treatment with 50 μM, 100 μM and 200 μM AmB ($P < 0.005$; 50 μM *vs.* 100 μM: $P = 0.8384$; 50 μM *vs.* 200 μM: $P = 0.0233$; 100 μM *vs.* 200 μM: $P = 0.0108$), a significant trend was observed between AmB dose and median survival ($P < 0.0001$), analysed by the log-rank test for trend. This indicates that treatment of cells with different AmB dosages affects non-apoptotic cell death significantly.

DMF *versus* bulk experiments

To validate the DMF platform for use in SCA, similar experiments were performed in bulk by following the protocol presented in Fig. 1C, which mimicked the protocol performed with the DMF setup. Yeast cells were subjected to treatment with different dosages of AmB and non-apoptotic cell death events were monitored using PI and fluorescence microscopy at the start (0 min) and the end (after 360 min) of treatment. In each experiment, at least 100 cells were analysed. In addition, cells were plated at these time points to analyse the number of dead cells. The fraction of apoptotic cells was then calculated by subtracting the number of PI-positive cells, assessed by fluorescence microscopy, and the number of living cells, *i.e.* the number of CFUs in the plating assay, from 100%.

As shown in Fig. 3, a dose-dependent increase in the subpopulation of non-apoptotic cells is obtained upon treatment with increasing doses of AmB. Moreover, 100% cell death is reached for all dosages of AmB after 360 min of treatment, as verified by CFU counting. These findings are in line with previous results which indicated that AmB induces 100% cell death in a yeast culture at a concentration of less than 5 μM, assessed by plating assay (data not shown). In addition, these results demonstrate that AmB indeed induces cell death *via* non-apoptotic and apoptotic mechanisms, which is in line with the literature.[33] Using low concentrations (*i.e.* less than 5 μM) of AmB, cell death is primarily caused by apoptosis and hence, cells are characterized as PI-negative.

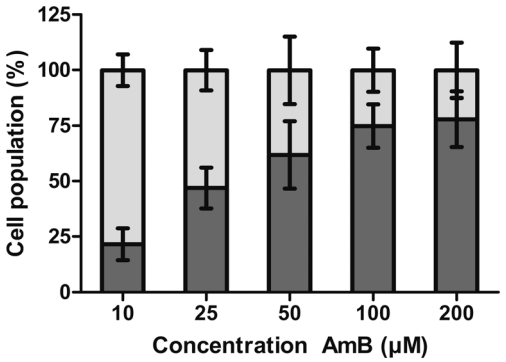

Fig. 3 Analysis of non-apoptotic and apoptotic fractions of cell populations upon treatment with AmB for 360 min in bulk. Yeast cells were treated with different dosages of AmB and at 0 min and 360 min, cells were analysed for membrane permeabilization events using PI and fluorescence microscopy and were plated to account for the apoptotic fraction. Means and sems (n = 3 independent biological repetitions) are presented. Dark grey bars represent the non-apoptotic fractions (PI+/growth−), and light grey bars represent the apoptotic fractions (PI−/growth−).

The results obtained in bulk were subsequently compared to those obtained on the DMF platform. To this end, the results generated by fluorescence microscopy after 360 min of AmB treatment were compared between both setups. The results of the plating assays were not used for comparison, as we only performed these assays in bulk. Plating assays on the DMF platform are not possible as we currently have no technique to individually remove seeded cells from the wells. In Fig. 4A, a correlation analysis is shown between the bulk and DMF data. A significant correlation ($P = 0.0015$) was found between the two setups, with a Pearson correlation coefficient of 0.97. It was also observed that the bulk experimental design is more susceptible to variations between repetitions than the DMF setup. A higher variation in the bulk results can be caused by, for example, more and extensive manual handling, which is not the case when the DMF platform is used. This is also reflected in the higher sems of the bulk results when compared to that of the DMF results in Fig. 4B.

In the lower AmB concentration range, the DMF platform appears to indicate a lower number of PI-positive cells as compared to the bulk analysis; however, the fraction of PI-positive cells in bulk does not significantly differ from the fraction of PI-positive cells on the DMF platform for any AmB dose tested and analysed after 360 min (Fig. 4B). This indicates that the DMF platform can potentially replace bulk analysis, thereby adding the advantage of conducting experiments with spatial and temporal resolution and with a much higher throughput as compared to bulk experiments. As such, this DMF platform offers an invaluable tool for more biologically oriented follow-up experiments. Regarding the antifungal effect of AmB, an extension of the presented comparative study in bulk and on the DMF setup (performed at an AmB incubation time of 360 min) over time can be included, which allows unravelling of the kinetics of AmB-induced membrane permeabilization.

Conclusion

In this article we have described DMF technology as a novel and automated tool for conducting single cell analysis (SCA) on non-adherent cells. Whereas conventional techniques that are often used for conducting SCA lack either spatial or temporal resolution, we presented a straightforward approach using the DMF platform to isolate single non-adherent cells and to monitor their dynamic responses at a defined position over time, in a well-controlled micro-environment. The

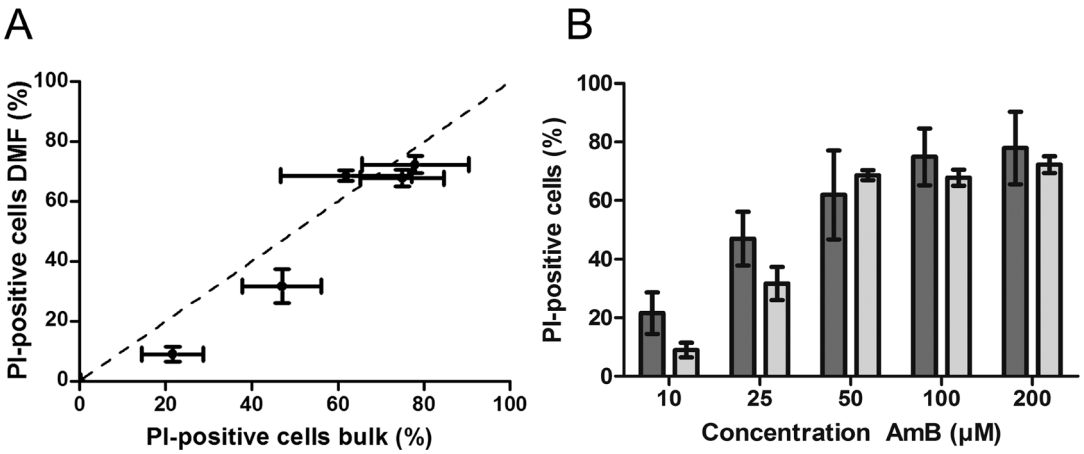

Fig. 4 Comparison of results obtained in bulk and on the DMF platform. (a) Correlation analysis between bulk and DMF results at 360 min. Means and sems are plotted (bulk: n = 3; DMF: n = 4). The Pearson correlation coefficient was found to be 0.97. The bisector is a guide to the eye and does not represent a linear fit of the data. (b) Representation of bulk (dark grey bars) and DMF (light grey bars) results at 360 min. Means and sems (n = 3 and n = 4) are plotted. No significant differences were found between bulk and DMF ($P < 0.05$). In all cases, n represents the number of independent biological repetitions.

spatio-temporal study in our work consisted of two parts; the generation of microwells ensured that trapped cells were located at a defined position during the experiments, *i.e.* spatial resolution, whereas temporal resolution was achieved by monitoring single cell responses in intermediate time intervals. To avoid osmotic lysis of cells, the DMF platform offered a unique possibility to seal the femtoliter droplets with oil. No external forces, other than surface tension and the physical forces generated by moving the droplet, were utilized to seed single cells inside the microwells, thereby avoiding cell damage. In the DMF experiments, we targeted yeast cells with a size of 4.5–5.5 μm, since the majority of cells within a yeast cell population are within that range. As such, either one or no cell is trapped in each microwell. In the bulk assays, no subpopulation of cells was targeted. As no significant differences were found between the bulk and DMF results, we can conclude that targeting the specified subpopulation of yeast cells did not affect our results. As such, the DMF technology holds great potential as a platform for assessing, for example, the killing kinetics of antifungal agents at single cell resolution.

As a proof of concept, the effect of different AmB dosages on membrane permeabilization events in yeast cells was investigated over time. We observed a dose-dependent response to the number of membrane permeabilization events. In addition, higher dosages of AmB (200 μM) caused more rapid membrane permeabilization than low AmB dosages (<50 μM), indicating that monitoring the cells over time is valuable for screening purposes towards identification of fast-killing agents. The DMF platform was validated by bulk experiments mimicking the DMF experimental design. A significant correlation was found between the bulk and the DMF platform, indicating that the DMF platform can be used for SCA without causing additional stress to the cells, as similar results were obtained in both setups. Moreover, the DMF platform can potentially replace bulk analysis, thereby conducting experiments with spatial and temporal resolution and with a much higher throughput as compared to bulk experiments. In addition, cellular heterogeneity can be studied thoroughly using the DMF platform, as we observed differential responses within a specific cell population. For instance, we observed that at a certain AmB dose and at a certain time point, some cells displayed membrane permeabilization, whereas others did not and this ratio fluctuated over time.

Although we only present the data obtained for membrane permeabilization of yeast cells during treatment, this platform can be further extended for analysis of the behaviour of cells in a multiplexed manner with regard to other features that play a role in cellular mechanisms, such as the production of reactive oxygen species and caspase activation. As such, different markers can be monitored simultaneously in individual cells at single cell resolution. In addition, incorporation of multiple microwell arrays for trapping of single cells can further improve the throughput and efficiency of the DMF platform. This would extend the possibility of challenging each set of cells with different drug concentrations, as well as analysing each array for different markers simultaneously. In conclusion, the DMF platform is an attractive tool for researchers interested in cellular processes and for unravelling the mode of action of antifungal agents.

Acknowledgements

In loving memory of my brother Jairaj. This research was financially supported by the KU Leuven Research Council (DBOF-grant P.T.K., OT/13/058 and IDO/10/012), the Flemish Institute for the Promotion of Innovation through Science and Development (IWT grant), and the European Commission's Seventh Framework Program (FP7/2007-2013) under the grant agreement BIOMAX (project no. 264737). This work was further supported by Industrial Research Fund, KU Leuven

(IOF/KP/12/002). K. T. and K. V. acknowledge the receipt of a post-doctoral grant from Industrial Research Fund, KU Leuven, and a pre-doctoral grant from IWT-Vlaanderen, respectively.

References

1 S. J. Altschuler and L. F. Wu, *Cell*, 2010, **141**, 559–563.
2 R. R. Jahan-Tigh, C. Ryan, G. Obermoser and K. Schwarzenberger, *J. Invest. Dermatol.*, 2012, **132**, 282.
3 T. Ramahaleo, R. Morillon, J. Alexandre and J. P. Lassalles, *Plant Physiol.*, 1999, **119**, 885–896.
4 J. Nilsson, M. Evander, B. Hammarstrom and T. Laurell, *Anal. Chim. Acta*, 2009, **649**, 141–157.
5 H. Yun, K. Kim and W. G. Lee, *Biofabrication*, 2013, **5**, 1758–5082.
6 M. Yang, C. W. Li and J. Yang, *Anal. Chem.*, 2002, **74**, 3991–4001.
7 A. R. Wheeler, W. R. Throndset, R. J. Whelan, A. M. Leach, R. N. Zare, Y. H. Liao, K. Farrell, I. D. Manger and A. Daridon, *Anal. Chem.*, 2003, **75**, 3581–3586.
8 A. Banaeiyan, D. Ahmadpour, C. Adiels and M. Goksör, *Micromachines*, 2013, **4**, 414–430.
9 D. Di Carlo, N. Aghdam and L. P. Lee, *Anal. Chem.*, 2006, **78**, 4925–4930.
10 D. Wlodkowic, S. Faley, M. Zagnoni, J. P. Wikswo and J. M. Cooper, *Anal. Chem.*, 2009, **81**, 5517–5523.
11 B. L. Wang, A. Ghaderi, H. Zhou, J. Agresti, D. A. Weitz, G. R. Fink and G. Stephanopoulos, *Nat. Biotechnol.*, 2014, **32**, 473–478.
12 S. H. Kim, T. Yamamoto, D. Fourmy and T. Fujii, *Small*, 2011, **7**, 3239–3247.
13 X. Wang, S. Chen, M. Kong, Z. Wang, K. D. Costa, R. A. Li and D. Sun, *Lab Chip*, 2011, **11**, 3656–3662.
14 H. Lee, A. M. Purdon and R. M. Westervelt, *IEEE Trans. Magn.*, 2004, **40**, 2991–2993.
15 T. Lehnert, M. A. M. Gijs, R. Netzer and U. Bischoff, *Appl. Phys. Lett.*, 2002, **81**, 5063–5065.
16 J. Voldman, R. A. Braff, M. Toner, M. L. Gray and M. A. Schmidt, *Biophys. J.*, 2001, **80**, 531–541.
17 S. K. Ameri, P. K. Singh, M. R. Dokmeci, A. Khademhosseini, Q. Xu and S. R. Sonkusale, *Biosens. Bioelectron.*, 2014, **54**, 462–467.
18 Z. Zhu, O. Frey, D. S. Ottoz, F. Rudolf and A. Hierlemann, *Lab Chip*, 2012, **12**, 906–915.
19 D. G. Grier, *Nature*, 2003, **424**, 810–816.
20 J. Enger, M. Goksor, K. Ramser, P. Hagberg and D. Hanstorp, *Lab Chip*, 2004, **4**, 196–200.
21 X. T. Zheng, L. Yu, P. Li, H. Dong, Y. Wang, Y. Liu and C. M. Li, *Adv. Drug Delivery Rev.*, 2013, **65**, 1556–1574.
22 V. Lecault, M. Vaninsberghe, S. Sekulovic, D. J. Knapp, S. Wohrer, W. Bowden, F. Viel, T. McLaughlin, A. Jarandehei, M. Miller, D. Falconnet, A. K. White, D. G. Kent, M. R. Copley, F. Taghipour, C. J. Eaves, R. K. Humphries, J. M. Piret and C. L. Hansen, *Nat. Methods*, 2011, **8**, 581–586.
23 V. Lecault, A. K. White, A. Singhal and C. L. Hansen, *Curr. Opin. Chem. Biol.*, 2012, **16**, 381–390.
24 H. M. Wyss, D. L. Blair, J. F. Morris, H. A. Stone and D. A. Weitz, *Phys. Rev. E: Stat., Nonlinear, Soft Matter Phys.*, 2006, **74**, 11.
25 M. Kuhnemund, D. Witters, M. Nilsson and J. Lammertyn, *Lab Chip*, 2014, **14**, 2983–2992.
26 G. J. Shah, A. T. Ohta, E. P. Chiou, M. C. Wu and C. J. Kim, *Lab Chip*, 2009, **9**, 1732–1739.
27 P. T. Kumar, F. Toffalini, D. Witters, S. Vermeir, F. Rolland, M. L. A. T. M. Hertog, B. M. Nicolaï, R. Puers, A. Geeraerd and J. Lammertyn, *Sens. Actuators, B*, 2014, **199**, 479–487.
28 A. Rival, D. Jary, C. Delattre, Y. Fouillet, G. Castellan, A. Bellemin-Comte and X. Gidrol, *Lab Chip*, 2014, **14**, 3739–3749.
29 S. C. Shih, P. C. Gach, J. Sustarich, B. A. Simmons, P. D. Adams, S. Singh and A. K. Singh, *Lab Chip*, 2014, **15**, 225–236.
30 D. Witters, K. Knez, F. Ceyssens, R. Puers and J. Lammertyn, *Lab Chip*, 2013, **13**, 2047–2054.
31 S. Elmore, *Toxicol. Pathol.*, 2007, **35**, 495–516.
32 F. Madeo, E. Frohlich and K. U. Frohlich, *J. Cell Biol.*, 1997, **139**, 729–734.
33 A. J. Phillips, I. Sudbery and M. Ramsdale, *Proc. Natl. Acad. Sci. U. S. A.*, 2003, **100**, 14327–14332.
34 D. Kleinbaum and M. Klein, *Survival Analysis- A Self-learning Text*, Springer, 2005.
35 D. Collett, *Modelling Survival Data in Medical Research*, Chapman and Hall/CRC, 2003.
36 M. Park, J. Hur, K. Kwon, J. Park, S.-H. Park and K. Suh, in *World Congress on Medical Physics and Biomedical Engineering 2006*, ed. R. Magjarevic and J. H. Nagel, Springer Berlin Heidelberg, 2007, ch. 70, vol. 14, pp. 246–249.
37 Y. Zhan, D. N. Loufakis, N. Bao and C. Lu, *Lab Chip*, 2012, **12**, 5063–5068.
38 L. Bergman, in *Two-Hybrid Systems*, ed. P. MacDonald, Humana Press, 2001, ch. 2, vol. 177, pp. 9–14.
39 J. Warringer and A. Blomberg, *Yeast*, 2003, **20**, 53–67.
40 K. C. Gray, D. S. Palacios, I. Dailey, M. M. Endo, B. E. Uno, B. C. Wilcock and M. D. Burke, *Proc. Natl. Acad. Sci. U. S. A.*, 2012, **109**, 2234–2239.
41 C. Riccardi and I. Nicoletti, *Nat. Protoc.*, 2006, **1**, 1458–1461.

